HHS Public Access

Author manuscript

Eur J Oral Sci. Author manuscript; available in PMC 2022 August 01.

Published in final edited form as:

Eur J Oral Sci. 2022 February ; 130(1): e12832. doi:10.1111/eos.12832.

Synthesis, characterization and evaluation of azobenzene nanogels for their antibacterial properties in adhesive dentistry

Rinku Trivedi[1], **Dixa Gautam**[1], **Gannon M. Kehe**[1], **Humberto D. Escobedo**[2], **Kruti Patel**[1], **Jeffrey W. Stansbury**[1,3,5], **Michael J. Schurr**[4], **Devatha P. Nair**[1,2,5]

[1]Department of Craniofacial Biology, University of Colorado Anschutz Medical Campus, Aurora, Colorado, USA

[2]Department of Pharmaceutical Science, Skaggs School of Pharmacy and Pharmaceutical Sciences, University of Colorado Anschutz Medical Campus, Aurora, Colorado, USA

[3]Department of Chemical and Biological Engineering, University of Colorado Boulder, Boulder, Colorado, USA

[4]Department of Immunology and Microbiology, University of Colorado Anschutz Medical Campus, Aurora, Colorado, USA

[5]Materials Science and Engineering Program, University of Colorado Boulder, Boulder, Colorado, USA

Abstract

The presence of cariogenic bacteria within the prepared tooth cavity at the adhesive resin-dentin interface is detrimental to the long-term stability and function of composite restorations. Here, we report the synthesis and incorporation of methacrylated azobenzene nanogels within bisphenol A-glycidyl methacrylate/hydroxyethyl methacrylate/ethanol (B/H/E) adhesive resins and evaluate their ability to reduce the bacterial invasion of cariogenic *Streptococcus mutans* biofilms while preserving the mechanical strength and structural integrity of the critical interfacial connection between the restoration and the tooth. The azobenzene nanogel, with a hydrodynamic radius of < 2 nm and a molecular weight of 12,000 Da, was polymerized within B/H/E adhesive formulations at concentrations of 0.5 wt.%, 1.5 wt.%, and 2.5 wt.%. While the double-bond conversion,

Correspondence Devatha Nair, 12800 E 19 Ave, P18-2401M, University of Colorado Denver, Aurora, CO 80045–2532, USA. Devatha.Nair@cuanschutz.edu.

Both Rinku Trivedi and Dixa Gautam contributed equally to the study.

AUTHOR CONTRIBUTIONS

Conceptualization: Devatha Nair, Dixa Gautam, Rinku Trivedi**; Methodology**: Rinku Trivedi, Kruti Patel, Humberto Escobedo, Jeffrey Stansbury, Dixa Gautam, Gannon Kehe, Michael Schurr**; Software**: Matt Barrows, Dixa Gautam, Gannon Kehe, Humberto Escobedo**; Validation**: Devatha Nair, Jeffery Stansbury**; Formal analysis**: Dixa Gautam, Gannon Kehe, Humberto Escobedo. Rinku Trivedi**; Investigation**: Dixa Gautam, Rinku Trivedi, Gannon Kehe, Kruti Patel, Humberto Escobedo, Alexis Mascarenas, Matt Barrows**; Resources**: Devatha Nair, Jeffery Stansbury, Clif Carey, Michael Schurr**; Data Curation**: Dixa Gautam, Rinku Trivedi, Gannon Kehe, Humberto Escobedo**; Writing-Original Draft Preparation**: Devatha Nair, Dixa Gautam, Rinku Trivedi, Gannon Kehe, Humberto Escobedo**; Writing-Review and Editing**: Devatha Nair, Dixa Gautam, Rinku Trivedi**; Visualization**: Dixa Gautam, Gannon Kehe, Humberto Escobedo, Devatha Nair**; Supervision**: Devatha Nair**; Project administration**: Devatha Nair**; Funding acquisition**: Devatha Nair and Michael Schurr.

CONFLICT OF INTERESTS

The authors declare that they have no conflicts of interest.

SUPPORTING INFORMATION

Additional supporting information may be found in the online version of the article at the publisher's website.

cytocompatibility, water solubility, and sorption of the adhesive networks were comparable, azobenzene nanogel networks showed improved hydrophobicity with a ≥ 25° increase in water contact angle. The polymerized adhesive surfaces formulated with azobenzene nanogels showed a 66% reduction in bacterial biofilms relative to the control while maintaining the mechanical properties and micro-tensile bond strength of the adhesive networks. The increased hydrophobicity and antibacterial activity are promising indicators that azobenzene nanogel additives have the potential to increase the durability and longevity of adhesive resins.

Keywords

caries resistance; composite; mechanical testing; nanoparticles; Streptococcus mutans

INTRODUCTION

Despite the popularity of composite dental restorations for their superior aesthetics and ease of application, the failure rate among methacrylate-based composites remains high [1, 2]. The replacement of existing restorations accounts for 50–70% of the over 200 million restorations placed each year and replacement dentistry costs more than $5 billion annually in the U.S. alone [3,4]. While adhesive dentistry has enabled less removal of the native tooth structure when performing restorations, placing the adhesive is a technique-sensitive venture, and poor adaptation to the surrounding tooth substance predisposes the adhesive-tooth interface to bacterial colonization [5]. Moreover, residual bacteria within the demineralized dentin weakens the interface, and this further provides a surface through which bacteria can then diffuse across freshly prepared dentin [6,7]. The failure to efficiently seal the dentin-adhesive interface leads to bacterial colonization by cariogenic bacteria at the tooth-restoration interface and is the main cause of secondary caries [8].

Among cariogenic bacteria, *Streptococcus mutans* (*S. mutans*) has been repeatedly identified as an important oral pathogen and early colonizer within the oral microbiome [9-11]. While it is not the only early colonizer present in the oral microbiome, the ability of *S. mutans* to generate a sticky, insoluble exopolysaccharide layer in the presence of dietary sugars makes the biofilm a particularly tough target to eliminate [12]. Over the years, several anti-bacterial compounds have been introduced within dental adhesives to combat biofilms and they include antibiotics, silver ions, and chlorhexidine [8]. The limited success of this approach can be attributed to concentration constraints and the variable diffusion kinetics of small molecules in the oral cavity [13]. Additionally, the inclusion and release of small molecule additives from the native polymer matrix have been known to have detrimental impacts on the mechanical strength of the restoration as a whole [14]. Over the past decade, the incorporation of methacrylated quaternary ammonium compounds within resins has been successful in reducing bacterial biofilm growth in the surface of composite restorations, although the concentration-dependent antibacterial impact of the adhesive must be balanced against the toxicity and loss of mechanical properties of the polymerized network [15,16].

Aromatic compounds (such as polyphenols, antimicrobial stilbenes, and azophenols) can prevent the growth of bacterial biofilms [17-19]. Azophenols belong to a class of compounds

classified as azobenzenes, which encompass a range of molecules that contain a core azo compound of two phenyl rings interconnected by an N = N linkage [20]. While the antibacterial activity of azophenols is often attributed to the ability of the phenolic groups to engage target receptors on bacterial membranes, the antibacterial properties of simple azobenzenes tethered via crosslinks within conventional dental polymer formulations has not been explored to date [21]. Azobenzene molecules are isomers that have distinct *trans* and *cis* conformations, with the energetically preferred resting *trans*-state observed to be considerably less polar and more hydrophobic than the *cis*-state of the molecule [20,22]. We hypothesized that a tethered azobenzene functionality within crosslinked adhesive dental polymer networks can increase the hydrophobicity of the network while eliciting an antimicrobial response. However, a major limitation of incorporating bulky, hydrophobic azobenzene networks within crosslinked networks is their insolubility in more hydrophilic solvents, such as ethanol. Our previous work has shown that prepolymerized amphiphilic nanogels canfunction as compatibilizers between hydrophobic and hydrophilic components within networks while preserving and/or enhancing the mechanical strength of the system [23,24]. Taking advantage of the synergistic properties of nanogels and azobenzene functionality, we have designed and formulated azobenzene-functionalized nanogels that can be incorporated within dental adhesive monomers. We hypothesize that, by incorporating azobenzene-functionalized methacrylated nanogels within ethanol-solvated, conventional BisGMA-HEMA dental resins (B/H/E), the *S. mutans* attachment and growth on dental adhesive networks will be inhibited while preserving the inherent strength of the dental adhesive network. The hypotheses to be tested are: (i) the incorporation of azobenzene-functionalized nanogels as additives within conventional dental resins will increase the hydrophobicity of the network while maintaining the mechanical performance of adhesive resins, and (ii) azobenzene-functionalized nanogels will reduce the presence of cariogenic bacteria on the modified resin substrates.

MATERIAL AND METHODS

Nanogel synthesis

The experimental design followed in this study is shown in Figure 1 and the monomers and initiators used in this study are shown in Figure 2A.

The monomers, 0.7 g of 4-hydroxyazobenzene and 0.56 g of hexamethylene diisocyanate, were homogeneously mixed in a 100 mL round bottom flask with a four-fold excess of toluene (all monomers and solvents were purchased from Sigma-Aldrich unless otherwise noted). A minimal amount of N, N-dimethylformamide (1 mL) was used to disperse the 0.7 g 4-hydroxyazobenzene, and 0.05 mL of dibutyltin dilaurate was added to initiate the alcohol-isocyanate reaction. Subsequently, 0.3 g of glycerol and 1 g of 2-isocyanatoethyl methacrylate (Monomer-Polymer and Dajac Labs) were added to the round bottom flask at the 10-min mark, and the solution polymerization was allowed to proceed at 20 ± 2°C for 12 h (Figure 2B). The amount of hexamethylene diisocyanate and 2-isocyanatoethyl methacrylate added to the reaction was calculated via a 1:1 functional group molar ratio of NCO to OH functionality from the monomers 4-hydroxyazobenzene and glycerol added to the system. The isocyanate–alcohol reaction was monitored with Fourier Transform-

Infrared Spectroscopy in mid-IR (Nicolet 6700; Thermo Scientific) and the disappearance of the OH and NCO peaks at 3650-3600 cm^{-1} and 2270 cm^{-1} were followed to ensure 100% conversion functional group conversion. The crude reaction mixture was purified by precipitation in ten-fold excess of hexane relative to the toluene volume via drop-wise addition. The precipitate was isolated, and the residual hexane was removed under reduced pressure. The resulting precipitates were suspended in dichloromethane and residual solvent was removed completely under vacuum to obtain the azobenzene nanogel.

Nanogel characterization

The molecular weight and size of the azobenzene nanogels were determined by triple-detector (refractive index, viscosity, light scattering) gel permeation chromatography (GPC max; Viscotek) in 0.35 μL/min tetrahydrofuran (EMD Millipore) as the mobile phase.

Azobenzene nanogel with or without B/H/E formulations

Control substrate formulated with bisphenol A glycerol dimethacrylate (BisGMA) (Esstech), 2-hydroxyethyl methacrylate (HEMA) (TCI America), and ethanol (Thermo Fisher Scientific) at 40:60:12 wt.% – hereafter referred to as B/H/E – was used in the study. The azobenzene nanogels were dispersed in the B/H/E at 3 different concentrations (0.5 wt.%, 1.5 wt.%, 2.5 wt.%). Camphorquinone (CQ) and ethyl 4-N,N-dimethylaminobenzoate (EDMAB) in the ratio 1:1, and at a concentration of 2 wt.% of the azobenzene nanogel/B/H/E formulation, were added as co-initiators. The CQ+EDMAB system is designated as I1 in this paper. Unless otherwise specified, the samples for material characterization were photocured with an LED curing light (Elipar DeepCure-S curing light; 3 M ESPE) for 2 min on each side at 700 mW/cm^2, to obtain high methacrylic double-bond conversions so that a meaningful comparison between the different test conditions could be carried out.

Viscosity

The viscosity of the formulations in the absence of polymerization initiators (n = 3) was studied using a cone-plate digital viscometer (CAP2000+; Brookfield) and the viscosity of azobenzene nanogel/B/H/E formulations in the presence and absence of the LED light exposure (60 s, 700 mW/cm^2) was noted.

Photoinitiating systems

Two photoinitiators were evaluated in this study. In addition to the photoinitiating system described above (CQ+EDMAB, designated as I1), we also evaluated a second dual-cure initiating system (I2) that consisted of both the photoinitiators CQ-EDMAB and the redox initiators benzoyl peroxide and dimethyl-p-toluidine. The azobenzene nanogel/B/H/E with CQ-EDMAB was divided equally by volume into separate vials and 4 wt.% of benzoyl peroxide was added to one vial, while 2 wt.% of dimethyl-p-toluidine was added to the second vial. The contents of the two vials were then mixed and exposed to light, thereby simultaneously initiating the redox and photoinitiators within the network. Irradiation was limited to two, 20 s exposures to the same LED light source, which represents a more clinically relevant timescale.

Degree of conversion

The degree of conversion for all formulations in the study was quantified with near-FTIR spectroscopy (Nicolet 6700; Thermo Scientific) by measuring the methacrylate peak area before and after polymerization at 6163 cm^{-1} (Resolution = 4 cm and Scans = 32). Samples were open cured in an elastomer mold (t = 0.9 mm, 80 μL) for measurements. The double-bond conversion was measured by the following equation:

$$Degree\ of\ Conversion \quad (\%) = \left(1 - \frac{A_{final}}{A_{initial}}\right) * 100$$

where $A_{initial}$ is the peak area before polymerization and A_{final} is the peak area after polymerization.

UV-Vis spectroscopy

Azobenzene molecules strongly absorb light between 300–500 nm in a concentration-dependent manner. Azobenzene nanogels dispersed in B/H/E formulation were quantified spectroscopically at concentrations of 0.5 wt.%, 1.5 wt.%,2.5 wt.%. The spectroscopy studies were performed on a 96-well plate using Biotek Synergy 4 microplate reader (BioTek Instruments), in which 20 μL azobenzene nanogel + B/H/E were added to each well plate (n = 3).

Contact angle, water solubility, and water sorption

The azobenzene nanogel was incorporated with B/H/E at 0.5, 1.5, and 2.5 wt.% relative to the B/H/E monomer/solvent content and polymerized to provide disc specimens (thickness = 1 mm, diameter = 5 mm, n = 3) that were used for the measurement of contact angle on a goniometer (Ossila). For contact angle measurements, one drop of water (15 μL) was placed on the surface of the disc and the angle at the interface was measured for each sample. For the solubility and sorption studies, the masses M_1, M_2, and M_3 were quantified. M_1 was the mass of samples immediately after polymerization on an analytical scale (Mettler-Toledo). The samples were sub-sequently stored in 10 mL distilled water at 37°C for 7 days. At the end of 7 days, the samples were carefully removed and gently and briefly blotted dry using Kimwipes (Kimtech Science) and the mass M_2 was noted. Subsequently, the samples were stored in a desiccator containing fresh silica gel packs in an incubator at 37°C for one week, after which mass M_3 was noted. The volume (V) of each specimen was measured in mm^3. Water solubility and sorption were calculated using the following formulae:

$$Water\ Solubility = \frac{M_1 - M_3}{v}$$
$$Water\ Sorption = \frac{M_2 - M_3}{v}$$

Cytotoxicity tests: 3-(4,5-dimethylthiazol-2-yl)-2,5-diphenyltetrazolium bromide assay (MTT)

For the elution cytotoxicity assay, the azobenzene nanogel/B/H/E discs (diameter = 10 mm, thickness = 0.9 mm, n = 3) were soaked briefly in ethanol and dried under a Cell Hood UV

lamp overnight for sterilization. The specimens were then soaked in 9 mL of Dulbecco's Modified Eagle's Medium (DMEM) and 100 μL of Penicillin-Streptomycin for 24 h at 37°C, 5 % CO_2, to uptake any extractable or unreacted monomer from the adhesive discs (Extract Media). After the 24-h incubation period, 1 mL (10%) of fetal bovine serum (FBS; Life Technologies) was added to the 9 mL of extract media. L929 mouse fibroblast cells (ECACC 85011425) were cultured at 37°C, 5 % CO_2, in 250 mL cell culture flasks until 90% confluence was achieved. Cells were treated with DMEM and 0.25 % trypsin for cell detachment. Cells were then pelleted via centrifugation and suspended in DMEM containing 10 % FBS and 1 % Penicillin-Streptomycin. The cell suspension was then seeded in a 96-well plate at a concentration of 3,375 cells per well and incubated at 37°C, 5 % CO_2, to reach 70% confluence. Subsequently, cell media was then aspirated and a series of dilutions (100, 50, 25, 12.5, 6.25, 0 % of extract media) of the media from the soaked specimens was added to the wells and incubated for an additional 24 h. The extracted media were then aspirated and the cells were washed with 1x phosphate buffered saline (PBS). The PBS wash was aspirated and 100 μL of DMEM containing 0.5 mg/mL of 3-(4,5-dimethylthiazol-2-yl)–2,5-diphenyltetrazolium bromide (MTT reagent) was added to each well and incubated for 4 h for the tetrazolium reduction to formazan crystals by the dehydrogenases contained within the mitochondria of viable cells. After 4 h, 20% sodium dodecyl sulfate in 50% dimethylformamide was added to each well to lyse the cells and solubilize the formazan crystals for 20 h. A microplate reading of each well was taken at 570 nm and percent viability was determined by comparison of the optical density of the extract cultures to the 0 % extract culture [25].

$$Cell\ Viability\,(\%) = \frac{A_{Experimental\ Group}}{A_{Control\ Group}} * 100$$

Mechanical tests

The flexural modulus and flexural strength of azobenzene nanogel/B/H/E formulations (0.5 wt.%, 1.5 wt.%, 2.5 wt.%) were evaluated using bar specimens (n = 5) in three-point bending on Materials Testing Systems (MiniBionix II; MTS). Bars (25 mm x 2 mm x 2 mm) were polymerized sandwiched between glass slides within an elastomeric mold. The degree of conversion of all the bar specimens was calculated after photopolymerization by monitoring methacrylate conversion in the near-IR (6163 cm^{-1}) range before and after photocuring. The initiating conditions were chosen such that high conversion of bulk polymer substrates is obtained to make a meaningful analysis for the difference in properties. The bars were tested immediately after polymerization (n = 5) and again after storage in distilled water at 37°C for 7 days (n = 5).

Microtensile bond strength (μTSB)

Fifteen permanent molar teeth were used for the dentin bonding study using azobenzene nanogel/B/H/E formulations on a Materials Testing System (MiniBionix II; MTS). The teeth were mounted in acrylic resin and the occlusal enamel was cut to expose the dentin using a high-speed dental handpiece. Prepared teeth were subjected to acid etching with 37% phosphoric acid for 15 s and rinsed and dried. Subsequently, the azobenzene nanogel

layer was applied, followed by the B/H/E layer, and then air was blown gently over the tooth to ensure that the bonding agent and nanogel had been dispersed as a thin even layer over the tooth's etched surface. Composite buildups were constructed using Filtek Z-100 (3 M-ESPE). Two layers were applied (2 mm thick each) and cured for 2 min to attain a consistent double-bond conversions (> 90%). Consistent, high-double bond conversions were sought to be able to baseline the effect of azobenzene nanogel within the B/H/E networks, without the compounding effect of variable/low double-bond conversion. The tooth was cut into 4 sections using a slow-speed water-cooled diamond saw (Isomet; Buehler) and up to 4 bars were obtained from each molar by sectioning the bonded teeth. Bar specimens (n = 4) were tested using the MTS to determine the μTBS on samples immediately after they were prepared. Another set of identical samples was placed in distilled water at 37°C for 1 week and then tested for microtensile bond strength [25-27].

Antibacterial study

Azobenzene nanogels/B/H/E discs (diameter = 9.8 mm, thickness = 0.9 mm, n = 3) with varying concentrations of nanogels (0, 0.5, 1.5, 2.5 wt.%) were soaked briefly in ethanol and dried under a Cell Hood UV lamp overnight for sterilization. *S. mutans* (ATCC 25175) was grown in a 5 mL Brain Heart Infusion (BHI) medium statically at 37°C, 5 % CO_2, for 24 h. Subsequently, the liquid culture was diluted at 1:50 in BHI + 1 % sucrose and seeded onto the adhesive discs and then placed in an incubator at 37°C. The optical density of the cultures was monitored via a Biotek Synergy 4 (manufacturer) microplate reader at 600 nm. After 10 h of culturing at 37°C, 5 % CO_2, the adhesive discs were removed, and the biofilms were removed via bath sonication for 15 min in 1x PBS . The PBS was serial diluted and plated on BHI agar plates for CFU quantification.

RESULTS

Nanogel synthesis and characterization

The azobenzene nanogel synthesis was monitored by following the degree of conversion of the NCO groups and the OH groups in mid-FTIR until 100% conversion was achieved (Figure S1). The molecular weight (Mw) and hydrodynamic radius (Rh) of the azobenzene nanogel were measured at 12,000 Da and 1.74 nm, respectively (Table S1).

The viscosity of azobenzene nanogel adhesive formulations

In the absence of polymerization initiators, the azobenzene nanogels that were added to the B/H/E at 0.5 wt.%, 1.5 wt.%, and 2.5 wt.% did not significantly alter the viscosity in comparison with the B/H/E control ($p < 0.05$). As the azobenzene molecule is also a photoisomer that absorbs light in the 300–500 nm range, the viscosity of samples was measured both in the absence and presence of irradiation in comparison to a control (Figure 3A).

UV-Vis spectroscopy was studied to capture the concentration of azobenzene nanogel within the B/H/E system in comparison to the control. Azobenzene molecules strongly absorb light between 300 and 500 nm in a concentration-dependent manner. The azobenzene nanogel synthesized for this study and incorporated within B/H/E also absorbs light between 300

and 500 nm, which can be captured in the UV-Vis spectra. Figure 3B shows the correlation between the increases in area under the absorption curves as a function of increasing concentration of the incorporated at 0.5 wt.%, 1.5 wt.%, and 2.5 wt.% azobenzene nanogel in the network at both 325 and 450 nm.

Photoinitiating systems and degree of conversion

The photoinitiator (I1) and the dual-cure initiating system (I2) with a photoinitiator and a redox initiating system both showed > 97% C═C double-bond conversion of all azobenzene nanogels in B/H/E at concentrations of 0.5 wt.%, 1.5 wt.%, and 2.5 wt.% ($p < 0.05$), as shown in Table 1 and Figure S2.

Contact angle, solubility, and sorption measurements

The water contact angle measurements indicate that the presence of 0.5 wt.% azobenzene nanogel increased the contact angle by almost 30 degrees compared to the B/H/E control ($p < 0.0001$). Further increasing the azobenzene nanogel content to 1.5 wt.% and 2.5 wt.% did not produce a significant further increase of the contact angle ($p > 0.6$). The water solubility and the water sorption results of the azobenzene nanogel samples indicate that the presence of nanogels within the B/H/E formulations did not significantly impact the ability of the network to swell and retain water (Table 1).

Mechanical tests-flexure strength

The flexural strength tests of azobenzene nanogels/B/H/E samples were conducted immediately after polymerization (Figure 4A) and after being stored for 7 days in distilled water at 37°C (Figure 4B). The results showed that there was no statistically significant difference in flexural strength or modulus (One-way ANOVA; $p > 0.05$) under both test conditions.

*μ*TBS tests

The microtensile bond strength tests on tooth samples indicated that the presence of the azobenzene nanogel within B/H/E formulations preserved the bond strength of the adhesive formulations under two different testing conditions. In condition 1, bars were tested immediately after they were polymerized (Figure 5A) and in condition 2, bars were stored at 37°C for 7 days in distilled water before testing (Figure 5B). The controls and the azobenzene nanogel substrates had comparable bond strengths, and statistical analysis further confirmed that there was no significant difference, with p-values of 0.35 and 0.67 for bar tested within condition 1 and condition 2, respectively.

Cytotoxicity evaluation

The elution MTT assay demonstrated cell viability for all the azobenzene nanogel samples in comparison to the control. The control demonstrated viability at 98.7% ± 2.4%, while viability at 100.7% ± 1.2%, 100.7 % ± 0.7%, and 98.9 wt.% ± 0.9 wt.% was observed for the azobenzene nanogel/B/H/E samples at 0.5 wt.%, 1.5 wt.% and 2.5 wt.% azobenzene nanogel concentrations, respectively (Figure 6); no statistically significant differences among the groups were found.

Biofilm evaluation

The antibacterial biofilm assay showed that, at 10 h, there was significantly reduced *S. mutans* present on substrates in comparison to the control (Figure 7). The azobenzene nanogel/B/H/E formulations showed a reduction of ~ 66% of colony-forming units on the surface of the photopolymerized substrates in comparison to the conventional B/H/E control. One-Way ANOVA statistical analysis (with Tukey ad-hoc correction) resulted in a p-value < 0.0001 for the number of CFU for all azobenzene nanogel-containing adhesives compared to the control; this indicated a significant reduction in the viable biofilm formed due to the presence of the azobenzene nanogel substrates. There was no significant difference between the 0.5 wt.%, 1.5 wt.%, and 2.5 wt.% azobenzene nanogel substrates.

DISCUSSION

Azobenzene nanogels were incorporated within conventional BisGMA/HEMA/ethanol (B/H/E) formulations to assess their ability to enhance the surface hydrophobicity and antibacterial activity without compromising the mechanical strength and biocompatibility of conventional adhesive formulations. The rationale for selecting the concentrations of azobenzene nanogel within B/H/E was based on the solubility limits of the azobenzene nanogel within B/H/E. While concentrations of the azobenzene nanogel between 2.5 wt.% and 20 wt.% were seen to increase the viscosity and significantly hinder the photopolymerization of the B/H/E networks, concentrations of azobenzene nanogel ≥ 0.5 wt.% were required for the anti-bacterial activity. Therefore, azobenzene nanogel concentrations between $0.5 \leq x \leq 2.5$ wt.% were selected for this study. As azobenzenes are photodynamic molecules that can undergo cyclical *trans-cis-trans* isomerization in response to 400–500 nm light exposure, it was important to ascertain that the movement of the azobenzene nanogel did not significantly alter the viscosity of adhesive formulations upon light exposure. Our results indicate that the viscosity of the azobenzene nanogel formulations was comparable to that of the control. The increased viscosity in both the control and azobenzene nanogel formulation observed upon light exposure can be attributed to the ethanol evaporation from the formulations that are accelerated upon irradiation.

The incorporation of the azobenzene nanogel within B/H/E formulations at different concentrations was studied using UV-Visible spectroscopy. The increase in the area under the curve between 250 and 400 nm indicates the absorbance of the azobenzene molecules and is a measure of the concentration of azobenzenes incorporated within the substrates. In contrast to the control B/H/E substrates, substrates with azobenzene nanogel at 0.5 wt.%, 1.5 wt.%, and 2.5 wt.% of azobenzene nanogels within B/H/E formulations showed increasingly broader curves with a shoulder that extends well into the visible range, indicating the higher concentrations of azobenzene within the azobenzene nanogel/B/H/E formulations.

The degree of methacrylate double-bond conversion of the polymerized substrates was measured using FTIR by following the peak at 6163 cm^{-1}. The two initiating conditions chosen in this study I1 and I2 ensured high C═C conversion of the polymer substrates. It is important to demonstrate that high double-bond conversions can be achieved under clinically relevant curing conditions in order to maximize the translation potential of this approach. High double-bond conversions are also needed to make a meaningful analysis

of the difference in mechanical properties between the networks in to the study. While both initiating conditions attained very high conversions, the I1 photoinitiating systems with CQ/EDMAB took up to 4 min to achieve > 98 % conversion in the formulation with azobenzene nanogels present. The increased time to attain high conversions can be attributed to the ability of the azobenzene molecule to absorb light in the 400–500 nm range, which effectively competes with CQ absorption. A second initiating system that could attain similar high conversions within a clinically relevant timescale was developed to establish the translational potential of the azobenzene nanogel additives. The I2 dual-initiating system with two initiators, photoinitiator (CQ/EDMAB) and a redox initiator (benzoyl peroxide and dimethyl-p-toluidine), was formulated as a two-part system so that > 98 % methacrylate conversion could be observed upon two, 20 s light exposures from a dental curing lamp, thereby establishing that high conversion within the azobenzene nanogel substrates is attainable in clinically relevant timescales.

The contact angle measurement of the azobenzene nanogel samples in comparison with the B/H/E controls indicated that the presence of azobenzene nanogel made the networks significantly more hydrophobic, as evidenced by the dramatic increase in contact angles observed. As the resting *trans*-state of the azobenzene is hydrophobic in comparison to the transient *cis* state, this result was predicted. The water contact angle of unfilled dental adhesives is seen to be between 10–50 degrees and the addition of 0.5 wt.% of the azobenzene nanogel to the B/H/E substrates drives the network to the upper limit of acceptable hydrophilicity for dental adhesives [28]. The enhanced hydrophobicity of the network can increase the resistance of the surface to *S. mutans* bacterial biofilm formation attachment and proliferation [27]. The water sorption and solubility of the azobenzene nanogel substrates indicate that the addition of the azobenzene nanogel up to 2.5 wt.% did not alter the ability of the material to absorb or retain water in comparison to the control. Given that a maximum of 2.5 wt.% azobenzene nanogels was incorporated within the B/H/E network, it is evident that the low concentrations of azobenzene nanogels studied here did not have a significant effect on the inherent swelling properties of the control network at a high double-bond conversion of 98%. The negative values observed for the water solubility studies in both the control and azobenzene nanogel substrates showed that the water absorbed during storage led to an increase in the measured mass of the substrates, indicating that under the conditions tested, the water sorption was greater than the solubility.

The flexural strength tests of the azobenzene nanogel/B/H/E substrates indicate that the addition of azobenzene nanogel/B/H/E up to 2.5 wt.% did not compromise the inherent strength of the B/H/E substrates upon polymerization and subsequent aging. The μTBS results followed a similar trend, indicating that the azobenzene nanogel did not alter or weaken the crosslinked network formed by the B/H/E formulations. These results confirm that the low concentrations of additives used in this study are below the threshold to significantly alter the polymer network formation and mechanical properties of the B/H/E networks.

Cytotoxicity assays are often performed as the first step towards assessing the biocompatibility of adhesives and the elution cytotoxicity assay has been used as a more clinically relevant indicator of the toxicity of adhesive networks [29]. Once polymerized, the

leachables that can elute from the adhesives can be correlated to the double-bond conversion of the adhesive networks, and the higher double-bonds conversion observed in this study contributed to the observed biocompatibility of the azobenzene nanogel formulation in comparison to the control. Therefore, the adhesive with the azobenzene nanogel as an additive is deemed non-toxic and had no negative impacts on healthy cell metabolism.

As the mechanical performance and biocompatibility of the azobenzene nanogel/B/H/E samples were, at a minimum, comparable to those of the control B/H/E samples, the ability of the networks to prevent the attachment and proliferation of cariogenic *S. mutans* was studied. *S. mutans* is a noted early colonizer within the oral microbiome and it is hypothesized that the ability of *S. mutans* to form a thick and sticky exopolysaccharide layer facilitates the attachment and proliferation of additional cariogenic oral bacteria. The azobenzene nanogel/B/H/E formulations showed a reduction of ~66% at 4 standard-deviations of colony-forming units (CFU) on the surface of the photopolymerized substrates in comparison to the conventional B/H/E control, indicating that the azobenzene nanogel can reduce the growth and proliferation of *S. mutans* on the substrates at 10 h. The minimum threshold evaluated of 0.5 wt.% azobenzene nanogel was sufficient for the reduction of the biofilm and no significant difference was observed between the 0.5 wt%, 1.5 wt%, and 2.5 wt% azobenzene nanogel substrates. Likely, the enhanced hydrophobicity of the surface of the substrates, as seen by the increase in the surface contact angle, impairs *S. mutans* attachment and growth [30]. It has been shown that the bacterial surface of *S. mutans* is highly hydrophilic and displays a preference for higher bacterial adhesion to hydrophilic surfaces [31]. Further studies are required over a longer period to see the long-term impacts of *S. mutans* inhibition. As the enhanced hydrophobicity of the surface of the substrates can control the attachment and growth of cariogenic *S. mutans* biofilms, the azobenzene nanogel additives can potentially pave the way for protective non-cariogenic oral biofilms formation. Additionally, the cyclical *trans-cis-trans* photoisomerization of the azobenzene molecule can be used to disrupt biofilm formation as a result of periodic exposure to visible light wavelengths between 400–500 nm [32]. Such an event can further reduce subsequent infections and contribute to the delay, and even prevention, of the onset of dental caries [33-35].

Overall, the results indicate that azobenzene nanogels within conventional B/H/E formulations at low concentrations (between 0.5 wt.% and 2.5 wt.%) maintained the mechanical strength of the adhesive network while increasing the hydrophobicity of the polymerized surface. Additionally, the elution cytotoxicity assay indicates that the azobenzene nanogel is non-toxic and can significantly reduce the *S.mutans* present within biofilms. While further studies are required to ensure the long-term efficacy of azobenzene nanogels as additives to networks, the ability to incorporate azobenzene nanogels within dental adhesive formulations is a promising approach to modify its hydrophobicity and introduce antibacterial properties within dental materials while preserving the inherent mechanical strength and biocompatibility of the network.

Supplementary Material

Refer to Web version on PubMed Central for supplementary material.

ACKNOWLEDGEMENTS

Thanks to Matt Barrows for gel permeation chromatography characterization, Alexis Mascarenas for assisting in the MTS protocol, and Dr. Clif Carey for tooth samples. Devatha Nair acknowledges financial support from NIH-NIDCR (grant no. K25DE027418). Devatha Nair and Michael Schurr acknowledge support from NIH-R21 (grant no. R21AI154360).

REFERENCES

1. Spencer P, Ye Q, Song L, Parthasarathy R, Boone K, Misra A, et al. Threats to adhesive/dentin interfacial integrity and next generation bio-enabled multifunctional adhesives. J Biomed Mater Res B Appl Biomater. 2019;107:2673–83. [PubMed: 30895695]
2. Spencer P, Ye Q, Park J, Misra A, Bohaty BS, Singh V, et al. Durable Bonds at the adhesive/dentin interface: an impossible mission or simply a moving target? Braz Dent Sci. 2012;15:4–18. [PubMed: 24855586]
3. Mjör IA, Shen C, Eliasson ST, Richter S. Placement and replacement of restorations in general dental practice in Iceland. Oper Dent. 2002;27:117–23. [PubMed: 11931133]
4. Jokstad A, Bayne S, Blunck U, Tyas M, Wilson N. Quality of dental restorations: FDI commission project 2–95. Int Dent J. 2001;51:117–58. [PubMed: 11563679]
5. Meerbeek BV. Landuyt KV, De Munck J, Hashimoto M, Peumans M, Lambrechts P, et al. Technique-Sensitivity of Contemporary Adhesives. Dent Mater J. 2005;24:1–13. [PubMed: 15881200]
6. Cardoso MV, de Almeida Neves A, Mines A, Coutinho E, Van Landuyt K, De Munck J, et al. Current aspects on bonding effectiveness and stability in adhesive dentistry. Aust Dent J. 2011;56(Suppl 1):31–44. [PubMed: 21564114]
7. Ye Q, Spencer P, Wang Y, Misra A. Relationship of solvent to the photopolymerization process, properties, structure in model dentin adhesives. J Biomed Mater Res A. 2007;80:342–50. [PubMed: 17001655]
8. Cocco AR, De Oliveira Da Rosa WL, da Silva AF, Lund RG, Piva E. A systematic review about antibacterial monomers used in dental adhesive systems: Current status and further prospects. Dent Mater. 2015;31:1345–62. [PubMed: 26345999]
9. Zhang Z, Yu J, Yao C, Yang H, Huang C. New perspective to improve dentin–adhesive interface stability by using dimethyl sulfoxide wet-bonding and epigallocatechin-3-gallate. Dent Mater. 2020;36:1452–63. [PubMed: 32943231]
10. Spencer P, Ye Q, Misra A, Goncalves SEP, Laurence JS. Proteins, Pathogens, and Failure at the Composite-Tooth Interface. J Dent Res. 2014;93:1243–9. [PubMed: 25190266]
11. Kermanshahi S, Santerre JP, Cvitkovitch DG, Finer Y. Biodegradation of Resin-Dentin Interfaces Increases Bacterial Microleakage. J Den Res. 2010;89:996–1001.
12. Waters MS, Kundu S, Lin NJ, Lin-Gibson S. Microstructure and mechanical properties of in situ Streptococcus mutans biofilms. ACS Appl Mater. 2014;6:327–32.
13. Chan DC, Hu W, Chung KH, Larsen R, Jensen S, Cao Densen, et al. Reactions: Antibacterial and bioactive dental restorative materials: Do they really work? Am J Dent. 2018;31:32B–6B.
14. Liu Y, Tjäderhane L, Breschi L, Li N, Mao J, Pashley DH, et al. Limitations in bonding to dentin and experimental strategies to prevent bond degradation. J Dent Res. 2011;90:953–68. [PubMed: 21220360]
15. Song L, Sarikaya R, Ye Q, Misra A, Tamerler C, Spencer P, et al. Multifunctional monomer acts as co-initiator and crosslinker to provide autonomous strengthening with enhanced hydrolytic stability in dental adhesives. Dent Mater. 2020;36:284–95. [PubMed: 31806495]
16. Chen L, Suh BI, Yang J. Antibacterial dental restorative materials: A review. Am J Dent. 2018;31(Sp Is B):6B–12B.
17. Concilio S, Sessa L, Petrone AM, Porta A, Diana R, Iannelli P, et al. Structure modification of an active azo-compound as a route to new antimicrobial compounds. Molecules. 2017;22:875.
18. Concilio S, Qian Y, Wei J, Zhou C. Antimicrobial polymer films for food packaging. AIP Conf Proc. 2012;1459:256–58.

19. Mori DI, Schurr MJ, Nair DP. Selective Inhibition of Streptococci Biofilm Growth via a Hydroxylated Azobenzene Coating. Adv Mater Interfaces. 2020;7: 1–8.
20. Mahimwalla Z, Yager KG, Mamiya JI, Shishido A, Priimagi A, Barrett CJ. Azobenzene photomechanics: prospects and potential applications. Polym. 2012;69:967–1006.
21. Piotto S, Concilio S, Sessa L, Diana R, Torrens G, Juan C, et al. Synthesis and Antimicrobial Studies of New Antibacterial AzoCompounds Active against Staphylococcus aureus and Listeria monocytogenes. Molecules. 2017;22:0–9
22. Nair HA, Singh Rajawat G, Nagarsenker MS. Stimuli-responsive micelles: A nanoplatform for therapeutic and diagnostic applications. In: Grumezescu AM, editor. Drug Targeting and Stimuli Sensitive Drug Delivery Systems. Elsevier Inc. 2018;303–42.
23. Saraswathy M, Stansbury J, Nair D. Water dispersible siloxane nanogels: A novel technique to control surface characteristics and drug release kinetics. J Mater Chem B. 2016;4:5299–307. [PubMed: 32263610]
24. Escobedo HD, Stansbury JW, Nair DP. Photoreactive nanogels as versatile polymer networks with tunable in situ drug release kinetics. J Mech Behav Biomed Mater. 2020;108:103755. [PubMed: 32310108]
25. Penmetsa RKR, Sri Rekha A, Poppuri KC, Sai Prashanth P, Garapati S. An invitro evaluation of antibacterial properties of self etching dental adhesive systems. J Clin Diagnostic Res. 2014;8: 3
26. Liebermann A, Ilie N, Roos M, Stawarczyk B. Effect of storage medium and aging duration on mechanical properties of self-adhesive resin-based cements. J Appl Biomater Funct Mater. 2017;15:206–14.
27. Esteban Florez FL, Kraemer H, Hiers RD, Sacramento CM, Rondinone AJ, Silvério KG, et al. Sorption, solubility and cytotoxicity of novel antibacterial nanofilled dental adhesive resins. Sci Rep. 2020;10:1–9. [PubMed: 31913322]
28. Wang J, Yu Q, Yang Z. Effect of hydrophobic surface-treated fumed silica fillers on a one-bottle etch and rinse model dental adhesive. J Mater Sci Mater. Med. 2018;29:1–9.
29. Poskus LT, Lima R, Lima I, Guimarães J, da Silva E, Granjeiro J. Cytotoxicity of current adhesive systems in vitro testing on cell culture of L929 and balb/c 3T3 fibroblasts. Rev. Odonto Cienc 2009;24:129–34.
30. Satou J, Fukunaga A, Satou N, Shintani H, Okuda K. Streptococcal Adherence on Various Restorative Materials. J Dent Res. 1988;67:588–91. [PubMed: 3170897]
31. Arango-Santander S, Gonzalez C, Aguilar A, Cano A, Castro S, Sanchez-Garzon J, et al. Assessment of Streptococcus Mutans Adhesion to the Surface of Biomimetically-Modified Orthodontic Archwires. Coatings. 2020;10:201.
32. Kehe GM, Mori DI, Schurr MJ, Nair DP. Optically Responsive, Smart Anti-Bacterial Coatings via the Photofluidization of Azobenzenes. ACS Appl Matet Interfaces. 2019;11:1760–5.
33. Garcia SS, Blackledge MS, Michalek S, Su L, Ptacek T, Eipers P, et al. Targeting of Streptococcus mutans Biofilms by a Novel Small Molecule Prevents Dental Caries and Preserves the Oral Microbiome. J Dent Res. 2017;96:807–14. [PubMed: 28571487]
34. Kret J, Zhang Y, Herzberg MC. Streptococcal antagonism in oral biofilms: Streptococcus sanguinis and Streptococcus Gordonii interference with Streptococcus mutans. J Bacteriol. 2008;190:4632–40. [PubMed: 18441055]
35. Zhu J, Chen GY, Yu L, Xu Haolan, Lui X, Sun J. Mechanically Strong and Highly Stiff Supramolecular Polymer Composites Repairable at Ambient Conditions. CCS Chem. 2020;2:280–92.

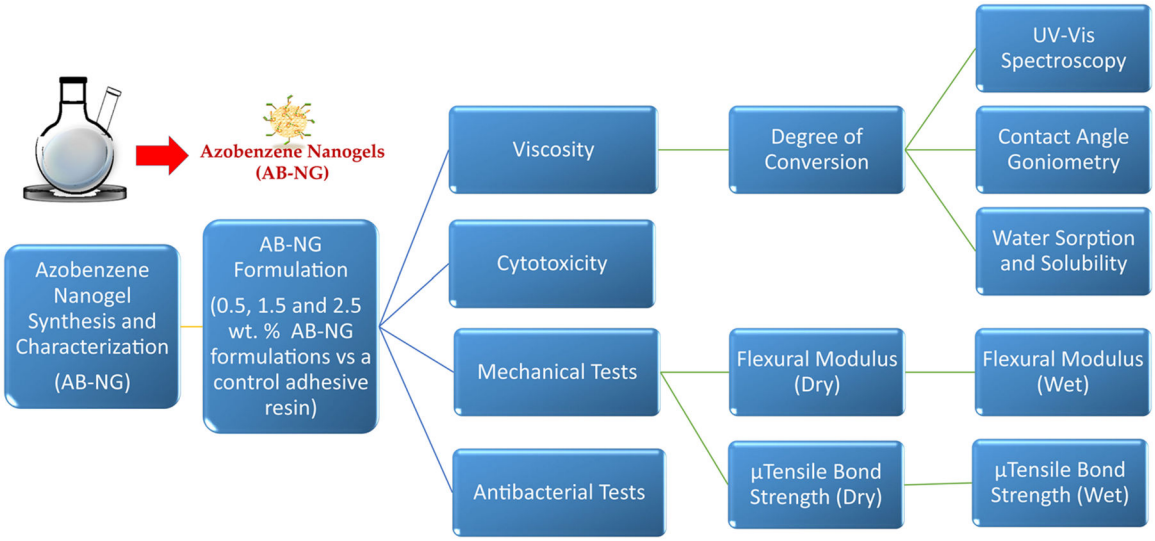

FIGURE 1.

The study design and experiments that were carried out in this work. The azobenzene nanogels (AB-NG) were synthesized and incorporated at 0.5 wt.%, 1.5 wt.%, and 2.5 wt.% within conventional BisGMA/HEMA/ethanol adhesive networks

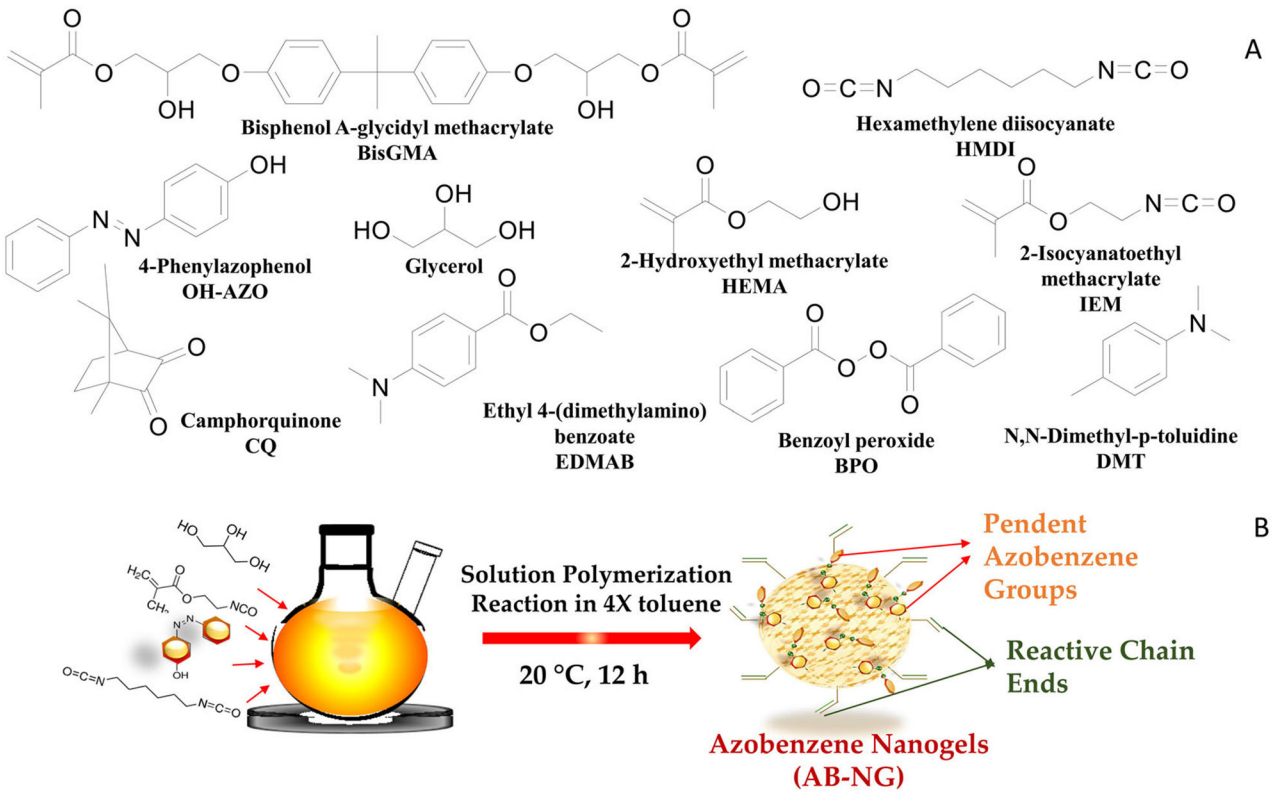

FIGURE 2.

The monomers and initiators used in the study (A). The azobenzene nanogel was synthesized using an isocyanate-alcohol solution polymerization protocol at 20°C (B)

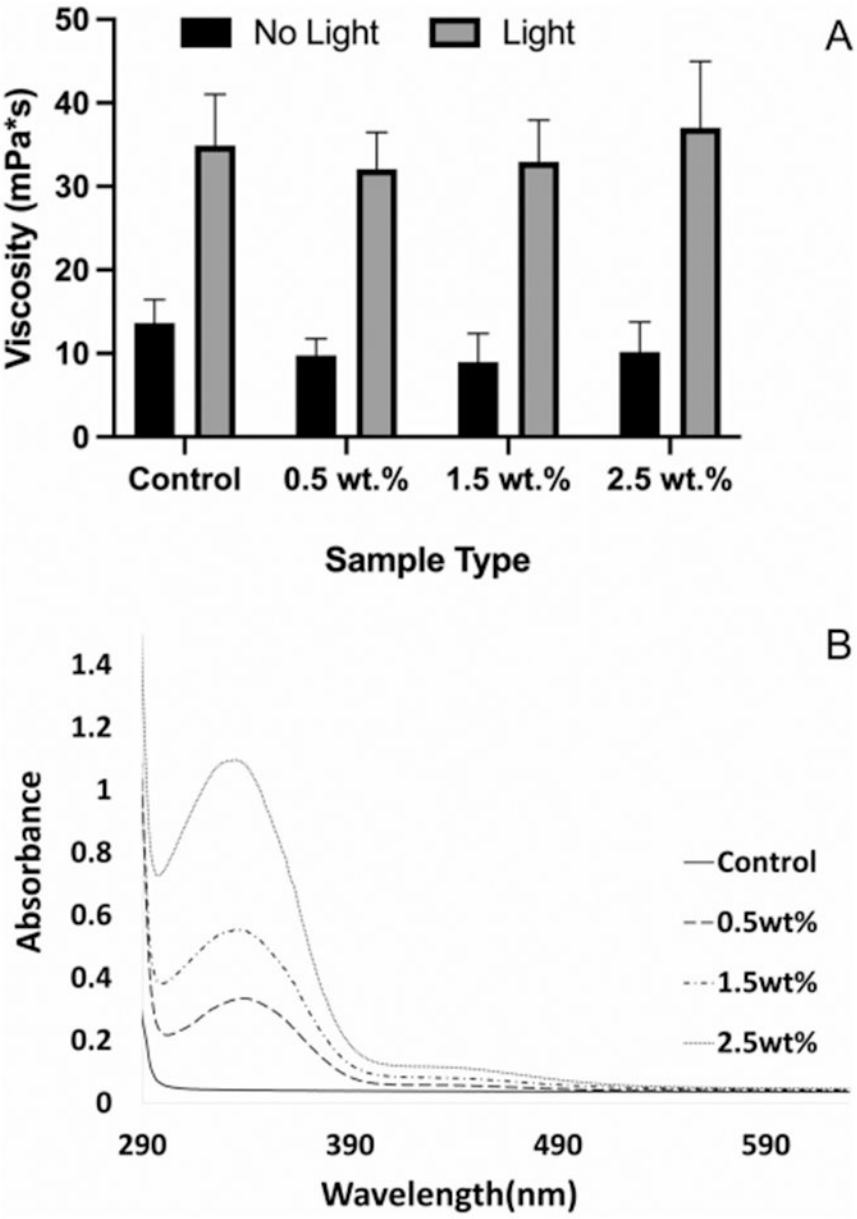

FIGURE 3.

The incorporation of azobenzene nanogel up to 2.5 wt.% did not impact the viscosity of the B/H/E in the absence or presence of light (A). UV-Vis spectroscopy quantifies the increasing concentration of azobenzene nanogel in the B/H/E formulations via the increased absorption observed between 300 and 450 nm (B). (Error bars denote the SD)

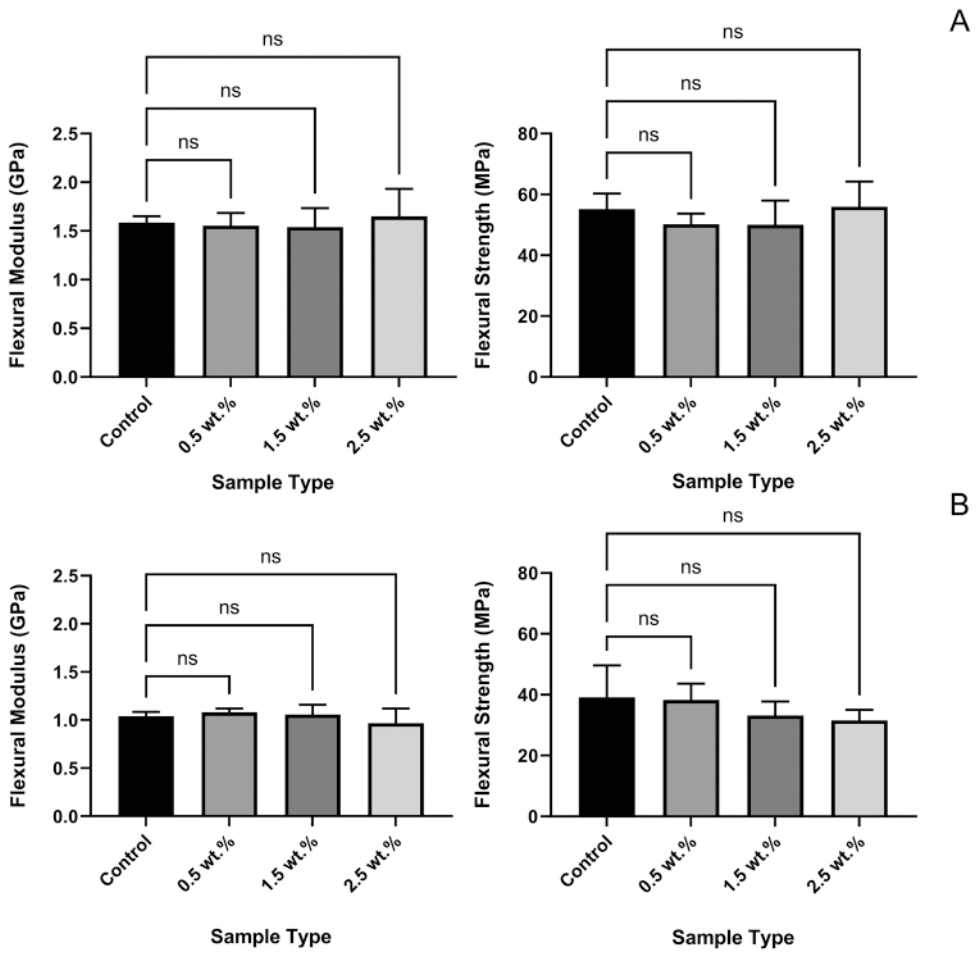

FIGURE 4.

Flexural modulus and flexural strenght tests in both conditions indicate that the mechanical strength of the material was retained in comparison to the control. Condition 1: immediately after applying the adhesive (A), and condition 2: at the end of 7 days in distilled water at 37°C (B). Mean values (Error bars denote the SD)

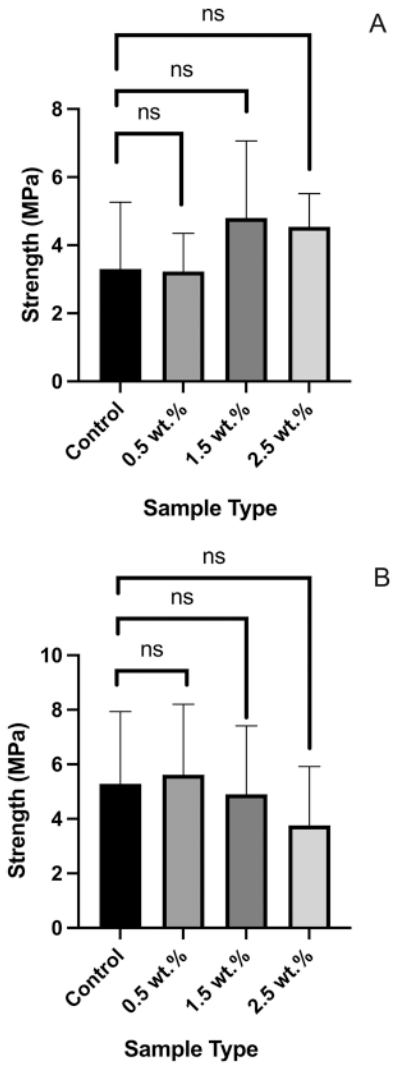

FIGURE 5.

The microtensile bond strength studies indicate that the strength of the azobenzene nanogel substrates is maintained in comparison to the control shown in both conditions. Condition 1: immediately after applying the adhesive (A), and condition 2: at the end of 7 days of storage in distilled water at 37°C (B). Mean values (Error bars denote the SD)

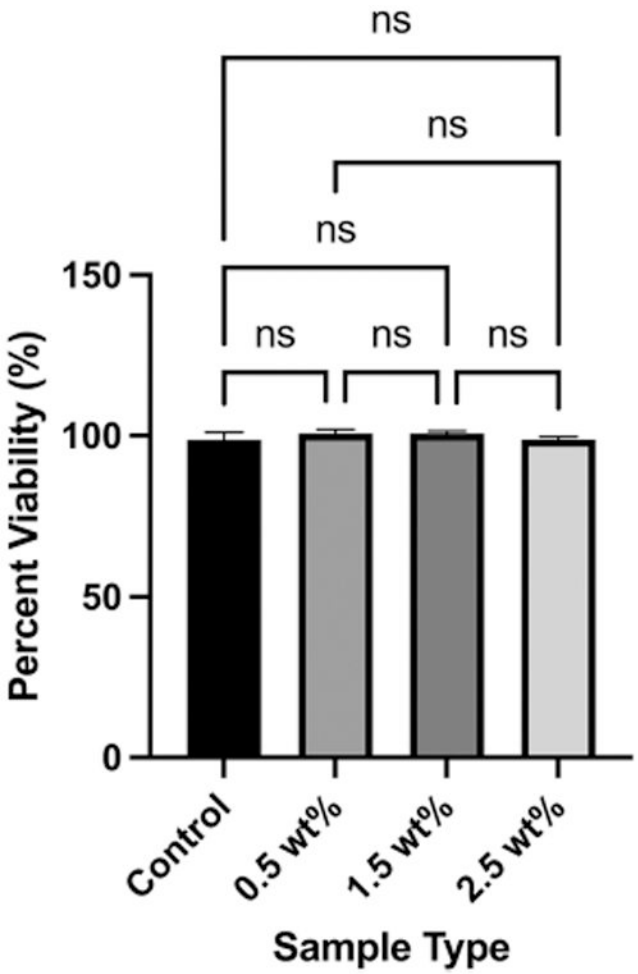

FIGURE 6.

The MTT assay demonstrates that cell viability upon exposure to different concentrations of azobenzene nanogel samples is comparable to the control adhesive formulation. Mean values (Error bars denote the SD)

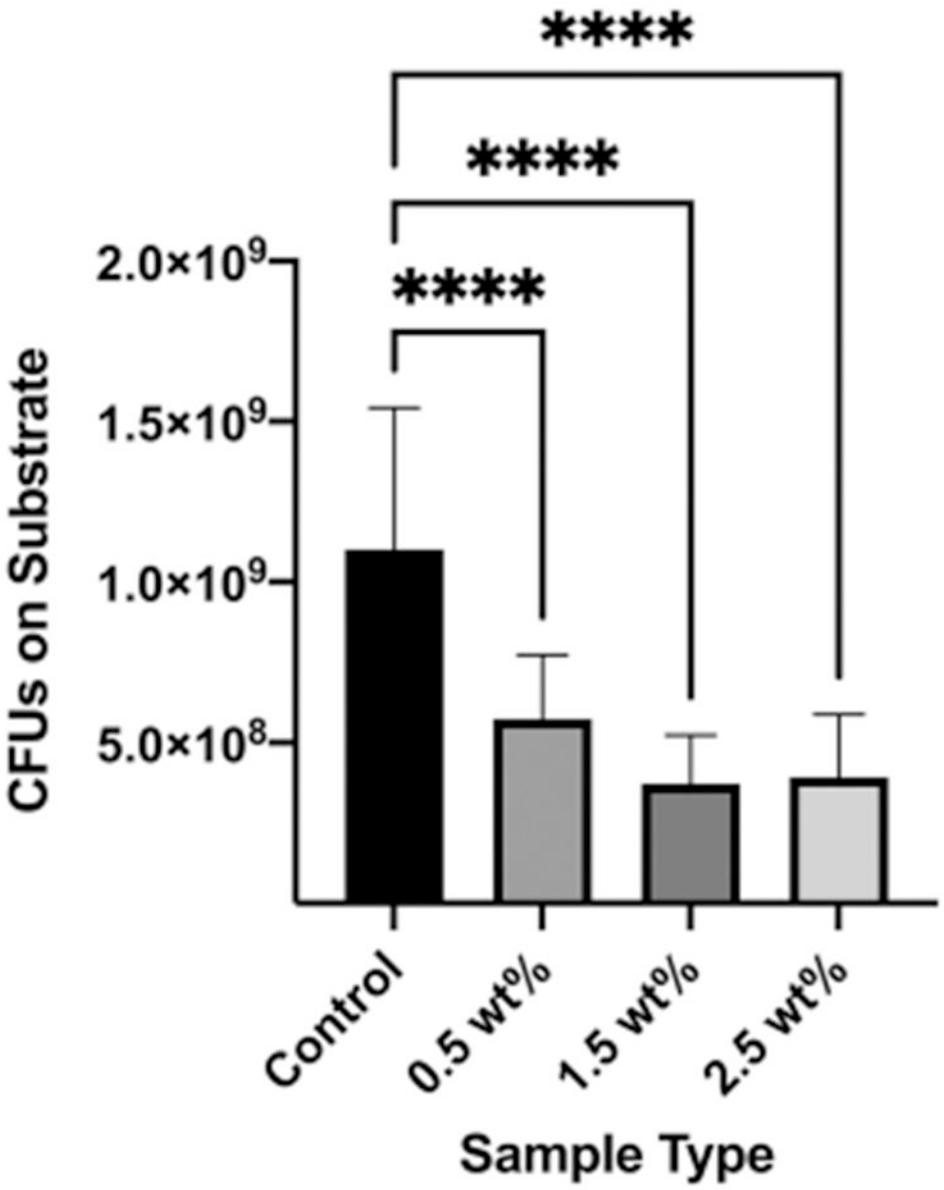

FIGURE 7.

Reduced *S. mutans* CFU on azobenzene nanogel substrates in comparison to the control. Mean values (Error bars denote the SD). ****$p < 0.0001$.

TABLE 1

Mean values (± SD) of the degree of conversion, contact angle, solubility, and sorption measurements

Sample type	Degree of Conversion I1 (%)	Degree of Conversion I2 (%)	Contact Angle (°)	Solubility ($\mu g/mm^3$)	Sorption ($\mu g/mm^3$)
Control	$97.3 \pm 1.06_a$	$98.6 \pm 0.3_b$	$28 \pm 1_c$	$-78 \pm 15_d$	$8 \pm 3_e$
0.5 wt.%	$96.7 \pm 0.81_a$	$98.6 \pm 0.3_b$	$56 \pm 6_c$	$-82 \pm 13_d$	$10 \pm 1_e$
1.5 wt.%	$97.9 \pm 1.04_a$	$98.0 \pm 0.2_b$	$58 \pm 2_c$	$-65 \pm 5_d$	$9 \pm 4_e$
2.5 wt.%	$97.6 \pm 0.6_a$	$98.2 \pm 0.5_b$	$53 \pm 2_c$	$-59 \pm 7_d$	$7 \pm 2_e$

Notes: I1 and I2 denote the two initiating systems studied. Values with the same lowercase letter down columns are not statistically significantly different ($p > 0.05$; Tukey's post-hoc test).